Critical analysis and optimisation of chromosome preparation and Fluorescence lifetime imaging microscopy: implications for DNA damage studies

Mohammed Yusuf[1,4*], Rosie Sanders[2], Sarah Berger[2], Rinyaporn Phengchat[3], Archana Bhartiya[4], Ian K. Robinson[4], Sylwia Kabacik[5], Stephen Barnard[5], Benji Bateman[2], Stanley W. Botchway[2*]

[1] The Rosalind Franklin Institute, Rutherford Appleton Laboratory Harwell Campus, Didcot, OX11 0QX

[2] Central Laser Facility, UKRI- Science and Technology Facilities Council, Rutherford Appleton Laboratory, Harwell Science and Innovation Campus, Oxfordshire, OX11 0QX, U.K.

[3] Quantum and Nanotechnology Research Centre, National Research Council of Canada, 11421 Saskatchewan Drive, Edmonton, AB, T6G 2M9, Canada.

[4] London Centre for Nanotechnology, University College London, London, WC1H 0AH UK

[5] UK Health Security Agency, Chilton, Oxfordshire OX11 0RQ

*Corresponding Author: E-mail: Stan.Botchway@stfc.ac.uk; mohammed.yusuf@rfi.ac.uk

Abstract:

Chromosome research is vital for cytogenetics, gene regulation as well as a myriad of vitally important aspects of organism health. The accurate preparation and analysis of human chromosomes is an important diagnostic procedure in clinical applications and medicine. Following a series of careful and critical chromosome preparation procedures and advanced imaging by fluorescence lifetime imaging microscopy (FLIM), we show that the current established method for chromosome preparation required further optimisation. The general standard fluorescence microscopy imaging of chromosomes does not inform on the overall preparation endpoint. We have applied FLIM as a critical analysis of the chromosome preparation process. Using immortalised (HEK293), cancer (HeLa) and primary cell lines (human T cell) and extracted chromosomes, we show that the overall excited state lifetime of their DNA labelled with fluorescence probes such as 4′,6-diamidino-2-phenylindole (DAPI) changes sufficiently to report on the sample preparation process and outcomes. The lifetime of DAPI when complexed with DNA changes from 3.2 and below 2.85 ns. Where such a significant reduction in lifetime is indicative of a poor chromosome preparation. The lifetime is affected by a range of factors including preparation drying time prior to staining as well as the mounting technique itself.

These new optimised conditions method was applied on chromosomes to investigate the effect of different x-ray irradiations on cells. We found a reduction in fluorescence lifetime at 0.5 Gy at arms and heteromorphic regions as compared with other irradiation doses (0.1, 1 Gy) and the control (0 Gy). We conclude that FLIM is an excellent method to allow improved and consistent chromosome preparation and analysis.

Keywords - Chromosomes, DAPI, FLIM, Multiphoton, Confocal, Imaging, T-Cells, HEK293, HeLa, X-rays, Radiation

Abbreviations

multicolour fluorescence *in situ* hybridization (mFISH)

methanol:acetic acid (MAA)

Fluorescence lifetime (FLT)

Fluorescence-lifetime imaging microscopy (FLIM)

UK Health Security Agency (UKHSA)

polyamine (PA)

4′,6-diamidino-2-phenylindole (DAPI)

Ethylenediaminetetraacetic acid EDta

Potassium chloride (KCL)

revolutions per minute (rpm)

Sodium chloride (NaCl)

hydochloric acid (HCl)

HEPES

TRIS

instrument response function (IRF)

chinese hamster ovary (CHO) cells

Introduction

Chromosomes store and transmit hereditary information including genetic variation. The preparation and analysis of human chromosomes i.e karyotyping is also an important diagnostic procedure in clinical applications and medicine where chromosomal instability and rearrangements are examined for the diagnosis of a number of haematological malignancies and prenatal/genetic medical disorders (Sumner, 1982, Tobias et al, 2011). Chromosome analysis often uses a variety of techniques, including karyotyping procedures such as Giemsa banding (G-banding); (Sumner, 1982) or multicolour fluorescence *in situ* hybridization (mFISH); (Yusuf et al, 2013; Bhartiya et al, 2021). Chromosome preparation for biological research and medicine is also critical in order to understand how genomes are organised and to furthermore examine several disease states including chromosomal DNA damage. Fluorescence imaging is seen as a standard tool in karyotyping and chromosome analysis. The most frequent method to study chromosome organisation and behaviour has been optical

microscopy. For this an accurate chromosome preparation procedure and visualisation is critical.

The routine process by which chromosomes are extracted from live cell cultures is well established (Rønne, 1990; Binz et al, 2024) and follows the procedure suggested by Hungerford (1965). This involves arresting cells in pro/metaphase state using mitotic inhibitors such as colecmid or nocodozole, respectively (Haraguchi et al, 1997). Following this the cells are burst using a hypotonic treatment that is required to swell the cellular volume from which the chromosomes are released from the cell's nuclei (Hsu, 1952; Makino and Nishimura, 1952; Hughes 1952). At this point chromosomes can be fixed to preserve chromosome spreads, most commonly methanol:acetic acid (MAA); (Sumner et al, 1973). This process is a significant step in obtaining and maintaining the well-defined chromosomal shape and distinct morphologies that we observe using an optical microscope e.g. karyotyping (Therman, 1980). Furthermore chromosomes can also be suspended into a polyamine buffer retaining both the proteins and nucleic acid when purified by standard procedures (Lewis and Laemmli, 1982) and are highly condensed (Yusuf et al, 2014). However, there is currently no available method to determine the efficiency of steps in the overall chromosome preparation process.

The use of excited state lifetime measurements of molecule is an important photophysical parameter that provides information about the environment such as molecular quenching (static or dynamic with other molecules), pH, Oxygen, energy relaxation, rotational dynamics, viscosity and energy transfer (Jana et al, 2016; Botchway et al, 2008; Clancy et al, 2023; Ahmed et al, 2021). Fluorescence lifetime (FLT) is defined as the average time a fluorophore remains in the excited state before emitting a photon and returning to the ground state. Fluorescence-lifetime imaging microscopy (FLIM) is the combination of lifetime measurements with fluorescence imaging. The fluorescence may be generated via one-photon or multiphoton excitation. The three key methods of generating excited state lifetime and the subsequent FLIM image are: (1) lifetimes frequency domain, (2) time-gating using a camera or (3) time-correlated single photon counting (TCSPC) combined with imaging methods. We have used the latter in this study and would thus focus on this technique. TCSPC requires pulsed excitation light source such as from a laser, a detector capable of discriminating single photons, an accurate timing device to synchronise the pulsed signal between the laser and detector, preferable to picosecond time resolution (Botchway et al, 2021). In the TCSPC-FLIM technique, a lifetime decay is obtained at the individual pixel-level, analysed using an exponential function and are colour-coded to produce images, Figure 1. FLIM is therefore a

powerful way to interrogate and visually inspect the overall chromosome preparation and outcome at the sub-micron resolution.

Chromosomal DNA damage can lead to a variety of conditions and related defects including genomic instability, mutation and cancer. Such damage may occur both endogenously and exogenously (Huang & Zhou, 2021). The former is a result of normal metabolism, hydrolysis, oxidation, alkylation, and mismatch of DNA bases. Whilst the latter may occur via both non- and ionizing radiation ultraviolet (UV) radiation as well as various chemicals agents. FLIM has also been used to investigate the structure and compaction state in mitotic chromosomes (Botchway et al, 2021; Estandarte et al, 2016) and represents a developing area of research. Chromatin compaction through different stages of mitosis has been studied with an increase in compaction seen at prometaphase to late anaphase and a decrease during telophase (Llères et al, 2009). Studies have shown that small molecules including cations and polyamines influence the conformation and compaction of chromatin (Visvanathan et al, 2013) such as Ca^{2+} that plays a crucial role in mitotic progression and condensation of chromosomes (Phengchat et al, 2016). The implications of this highlights the importance of chromosome research as a field, and therefore the optimisation of chromosome sample preparation.

Using the FLIM technique, we observe the sub-optimal effect of the overall chromosome process such as the fixation, drying and concentration of DNA labelling probes. A consistent lifetime of 3.2 is reduced to below 2.85 ns when any part of the process is altered to a less optimal condition. Furthermore, FLIM was used to show that ionising radiation of mammalian cells leads to certain parts of the chromosome being more sensitive to damage than others and displayed a shorter lifetime. The lifetime of the heteromorphic region of chromosome 1 in particular, is reduced from 2.7 ns to 2.1 ns (HeLa cells) and from 2.7 ns to 2.5 ns for (T cells) following 0.1 - 0.5 Gy irradiation.

Materials and Methods

A flowchart showing the complete chromosomes sample preparation procedure and live cell irradiation is shown in Figure 1.

Cell culture

HeLa (Henrietta Lacks) cells that are human cervical cancer cells (passage 5) were cultured in T75 flasks in phenol-red free DMEM media (Gibco, Life Technologies, UK) supplemented with 10% FBS (Gibco, Life Technologies, UK), 5 mM glutamine/1% glutamax (Gibco, Life Technologies, UK) and 1% penicillin-Streptomycin (Gibco, Life Technologies, UK) at 5% CO_2 at 37 °C. Chromosomes were prepared from flasks that were 70-80% confluent.

HEK293-cells that are originally derived from human embryonic kidney 293 cells were initially purchased from ECACC (UK). HEK293-cells were also grown in T75 flasks in phenol-red free DMEM media (Gibco, Life Technologies, UK) supplemented with 10% FBS (Gibco, Life Technologies, UK), 5 mM glutamine (Gibco, Life Technologies, UK), 5 mL sodium pyruvate (Gibco, Life Technologies, UK) and 1% penicillin-streptomycin (Gibco, Life Technologies, UK) at 37 °C with 5% humidity. Once the flasks were 70-80% confluent they were used for preparing chromosomes.

Human T-cells are a primary cell line that were extracted from a female blood donor provided by Dr Sylwia Kabacik at the UK Health and Security Agency. The extraction and growth of T-lymphocytes was done following the protocol outlined in Bhartiya *et al.* in 2021. The T-cells were incubated at 37 °C and 5% humidity at an angle of 10 ° from horizontal. They were then allowed to reach a density of approximately 3 x 10^5 cells per mL, at which point they were ready for chromosome preparation.

Non mammalian cell lines

Chinese hamster Ovary (CHO) cells, initially purchased from ECACC (UK), were grown in phenol red free Dulbecco's modified eagle medium nutrient mixture F-12 (DMEM F-12) (Gibco, Life Technologies, UK). DMEM F12 was supplemented with 10% FBS (Gibco, Life Technologies, UK) and 1% Penicillin-Streptomycin (Gibco, Life Technologies, UK). The cells were grown to 70-80% confluence in 5% CO2 at 37 °C and if required were split 1:12. Prior

to chromosome preparation cells were grown to a cell count of approximately 2 x 10^5 to 2.5 x 10^5 cells per mL.

Gerbil spleen cells were cultivated following the protocol described in Schain et al., 1995 to produce cells in suspension. Gerbil Spleen cells once extracted are stored in RPMI-1640 media (Gibco, Life Technologies, UK) supplemented with L-glutamine (Gibco, Life Technologies, UK) and 1% penicillin-streptomycin (Gibco, Life Technologies, UK). Chromosomes from this preparation were provided by Dr Thomas Brekke. Cells were cultured to a cell count of between 3 x 10^5 and 4 x 10^5 cells per mL prior to chromosome preparation.

X-ray Irradiation for Induction of Cellular DNA Damage

HeLa, HEK293 and human T-lymphocytes were irradiated with 0.1 Gy for 12 seconds, 0.5 Gy for 1 minute and 1 Gy for 2 minutes and at 0 Gy as a control using hard X-rays at a dose rate of 1.7 Gy/min at the UK Health Security Agency (UKHSA). The X-ray source used was 250 kVp, 13.0 mA at 500 mGy/min. (AGO X-Ray Ltd., West Coker, UK) fitted with both 1 mm copper and 1 mm aluminium filtering. Irradiations were performed at room temperature.

Chromosome Preparation and methanol acetic acid fixation

Chromosomes were prepared as previously described (Bhartiya *et al.* in 2021, Moralli et al, 2011; Yusuf et al, 2013). Once cell cultures were grown to correct confluency, 10 µg/mL colcemid (Thermofisher Scientific, UK) was added. The cells including the colcemid were incubated for up to 16 hours at 37 °C with 5% CO_2. After the incubation the cells were harvested for chromosome preparation. Adherent cell lines HeLa and Hek293 were trypsinised by adding 3 mLs of 10% trypsin-Ethylenediaminetetraacetic acid (EDTA); (Gibco, Life Technologies, UK) to the flask and incubating for 5 minutes in an incubator at 37 °C. Once the cells were in the solution, 3 mLs of cell media was added before cells were centrifuged at 1000 revolutions per minute (rpm) for 10 minutes. All cells were centrifuged and the supernatant was subsequently removed. Prewarmed (37 °C) 75 mM Potassium chloride (KCL); (VWR, UK); (hypotonic solution) was added dropwise to the pellet and the cells were left to incubate in a water bath at 37 °C for 10 minutes. The tubes were centrifuged at 1000 rpm for 10 minutes. Meanwhile, a 3:1 methanol (Scientific Laboratory Supplies, UK), acetic acid solution (Sigma-Aldrich, UK); (MAA) was prepared, this needs to be prepared freshly to be effective, as if left too long an MAA solution will react and undergo esterification. Once centrifuged, the

supernatant was once again removed from the pellet and MAA solution was added dropwise to the pellet, while vortexing, before centrifugation at 1000 rpm for 10 minutes. This washing process with MAA was repeated three times. The fixed samples were stable in the fixation buffer for several months at 4 °C.

Following irradiations, the media of cells was replaced with appropriate fresh media and placed back in the incubator at 37°C with humidified 5% CO_2. 0.15 to 0.2 µg/mL Colcemid (Thermofisher Scientific, UK) was added right after irradiation before placing the cells back in the incubator or between 7 hrs to 24 hr after irradiation.

Chromosome Mounting on Microscope Glass Slides

Prior to mounting, microscope slides were prepared by soaking them in 70% ethanol (Sigma-Aldrich, UK) overnight in order to remove any grease on the slides. They were wiped with high grade colourless soft tissues and placed in a -20 °C freezer for 30 minutes. Once cool, the slides were removed and humidified by gently blowing on them. At this point 20-30 µL of fixed chromosome preparation solution was dropped onto the slide from a height of approximately 30 cm. This protocol was used for mounting all the cell lines used in this study apart from human T-cells. Instead, human T-cells slides were suspended approximately 5 cm above the slide.

Polyamine chromosome isolation, decondensation and recondensation

Chromosomes were prepared as previously described (Hayashihara et al, 2008; Sone et al, 2002; Yusuf et al, 2014). HeLa cells were arrested at prometaphase using a combination of double thymidine block and nocodazole (Sigma, UK) at 2.5 mM and 0.1 µg/ml final concentration, respectively. Prometaphase HeLa cells were harvested at 6 h of nocodazole (Sigma, UK) treatment with mitotic shake-off. Chromosomes were isolated in-solution from the cells using polyamine (PA) buffer as follow: the cells were swollen in 75 mM KCl (VWR, UK) at 37 ºC for 15 min. The cell pellet was retrieved by centrifugation at 1200 rpm for 5 min then resuspended in PA buffer (15 mM Tris-hydochloric acid (HCl) (Sigma, UK), pH 7.2, 80 mM KCl (VWR, UK), 20 mM Sodium chloride (NaCl); (Sigma, UK), 2 mM EDTA (Sigma, UK), 0.2 mM spermine (Sigma, UK) and 0.5 mM spermidine (Sigma, UK) containing 0.12% digitonin (Sigma, UK). The cells were incubated on ice for 10 min, then followed by vortexing

vigorously for 2 min. The suspension was centrifuge at 190 xg for 3 min at 4 ºC to separate chromosomes from cell debris. The supernatant fraction containing chromosomes was collected and subjected to the second centrifugation at 1750 xg for 10 min at 4 ºC. The chromosome pellet was gently resuspended in 500 µl of PA buffer and stored at 4ºC.

For imaging, 'in-solution' isolated chromosomes above were further diluted with PA buffer at 1:40 dilution. Diluted chromosome solution was loaded into wells of a poly-l-lysine (0.01%); (Sigma, UK) coated 8-well glass chamber slides (150 µl per well). Chromosomes were allowed to settle down on ice for 15 min, followed by centrifugation at 400 xg for 10 min at 4 ºC. After centrifugation, chromosomes were stained with 4 µM DAPI (Thermo Fisher Scientific, UK) in PA buffer for 10 min at 4 ºC. This was then washed 3 times for 5 mins using a PA buffer. The chamber slides were placed under Nikon Ti-E or Ti2-E microscope, with an x60, NA 1.2 water immersion objective for lifetime observation with single photon. To decondense chromosomes, PA buffer was replaced with EDTA-HEPES buffer (10 mM EDTA (Sigma, UK) in 10 mM HEPES pH 7.4 (Sigma, UK). Lifetime data was collected at 10 mins after buffer exchange.

Chromosomal DNA Staining with DAPI, Hoechst and NuncBlue

All slides were dried before the staining process where 15 µL of 4 µM DAPI (Thermo Fisher Scientific, UK) was added to the centre of the slide. A coverslip was then added directly over the drop of DAPI (Thermo Fisher Scientific, UK) ensuring that the stain covered the coverslip area. DAPI was then left for the required time before imaging. A similar technique was used for other stains, that is 15 µL of 4 µM Hoechst 33258 (Thermofisher Scientific, UK) and 1 drop of NucBlue (Thermofisher Scientific, UK). Once the required stain was applied, the slides were stored in the dark.

Chromosome imaging by Epifluorescence microscopy Confocal and FLIM

It was found easier to image the chromosomes first using a fluorescence microscope (Zeiss Z2 Axio imager with Isis software) to identify the chromosome spreads prior to the confocal and FLIM imaging. Using a 10 x objective, the entire chromosome slides were scanned and the position of chromosome spreads were recorded. Next, a 60x (water or oil) microscope objective was used to obtain higher magnification of a chromosome spread. This same chromosome spread was then imaged using the confocal with FLIM acquisition. The setup used in this work has already been described in previous literature (Botchway et al, 2015). Briefly for single-

photon excitation a blue 405 nm laser (Becker & Hickl) was used. Imaging was carried out on a Nikon Ti-E or Ti2-E microscope, with an x60, NA 1.2 water immersion objective. A Nikon EC2 was used to raster-scan the laser, and the fluorescence was collected using the same objective. Fluorescence was detected using a hybrid photomultipler tube detector (one HPM100-40, Becker and Hickl). A bandpass filter (460/60) and together with a long-pass filter (FL450, Thorlabs) was used to filter out the laser.

For the FLIM acquisition, the same confocal setup was used together with a Becker and Hickl SPC830 or a SPC-QC 104 computer controlled module. These were controlled by a SPCM (version 9.0, 64 bit) data acquisition software. The pixel number for the confocal and FLIM acquisition was set to a minimum of 256 x 256 or 512 x 512 The image is then acquired using the FiFo mode, which acquires individual photon and assigns a xy coordinate (and arrival time) then stores the data on the TCSPC PC card. FLIM setup can be seen in Figure 2.

TCSPC and FLIM calibrations

Prior to FLIM data acquisition the instrument response function (IRF) was determined, to account for noise introduced by the electronics and laser fluctuations that may lead to complex excitation pulse profile. Moreover, the set-up was calibrated with known fluorophores, such as 1 μM fluorescein, rhodamine B, 7-hydroxycoumarin carboxylic acid in water with well characterised and known lifetimes. Experimentation only proceeded when fluorescent lifetime measurements were within 5% of literature values (Ahmed et al, 2021).

FLIM SPCImage software analysis

Following the data acquisition, FLIM images were processed using the SPCImage software version 8 (Becker and Hickl). The first step in the data analysis is to set a threshold so that pixels with low photon counts (less than 100 Ph/s in the peak channel are discarded). Typically, the threshold is set to between 25 and 35 for initial peak of 100), with the exact threshold being determined by the level of the background signal. The main aim of this step is only to analyse pixels that have photon counts above the set threshold using equation 1. Next, the model is set based on the decay curve shown, with the majority of FLIM readings requiring 'incomplete multiexponentials' due to the long FLT, and a repetition time of 12.5 ns is set off the 80 MHz laser. When the laser repetition rate can be varied, this incomplete decay analysis is no longer necessary. Where an average count of 100 is seen for most of the pixel binning up to 3 times may be applied to increase the photon count for the analysis. However, this has the effect of reducing the overall resolution of the FLIM image. The data points are fitted to a maximum-

likelihood estimation model. The next parameter tested for is the chi-squared value that needs to be 0.9 – 1.3, as this is a measure of goodness of fit. Therefore, a chi-squared value of >1.3 suggests there are multiple lifetime components, whereas <0.8 may indicate a poor fit of the data. Both of which indicate that the data requires further and careful interpretation. The decay fitting for every pixel in the image generates a mean histogram lifetime distribution as well as individual distribution and FLT values for each pixel. A false-colour range may also be generated to allow comparison of different chromosome spreads.

Equation 1

$$I(t) = \sum_{i=1}^{n} \alpha_i exp\left(-\frac{t}{\tau_i}\right)$$

$$\tau_{ave} = \sum \alpha_i \tau_i$$

Results and Discussion

Investigating the sensitivity of different fluorescent stains for fluorescence lifetime imaging microscopy of chromosomes

The use of DAPI for fluorescence imaging is well established for chromosome imaging (Bhartiya et al, 2021; Botchway et al, 2021; Estandarte et al, 2016). It is a fluorescent stain that binds strongly to DNA A-T minor groove (Tanious et al, 1992). Moreover, DAPI has been shown previously by Estandarte *et al.* in 2016 to give a strong difference in FLT between the heteromorphic regions of specific chromosomes, i.e 1. Here we compared the effectiveness of other DNA stains to determine any improvement in the current experimental protocol and the advantage offered by lifetime imaging to characterise the method effectiveness.

We initially tested Hoechst 33258 as an alternative to DAPI and FLT measurements. Both Hoechst 33258 and DAPI bind to the minor groove of DNA and favour AT rich regions (Cavatorta et al, 1985; Portugal and Waring, 1988) as mentioned above. However, there are some key differences between Hoechst and DAPI, one of which is a greater cell permeability by Hoechst (Breusegem et al, 2002) so that it is used mostly for live cell imaging. This could improve the ability of Hoechst to stain the chromosome spreads and improve the signal (photon

count) obtained from FLIM images. However, following FLIM data acquisition for equimolar probes (4 µM Hoechst and 4 µM DAPI), it was found that Hoechst resulted in a lifetime of 2.1 ns with no clear arm to centromere lifetime difference, whereas the changes found for DAPI showed a clear arm (3.1 ns) and centromere (2.6 ns) lifetime differences (Figure 3B and C, Supplementary table 1). This suggests that DAPI is a better chromosome stain to use for detecting FLT changes in chromosome preparation than Hoechst 33258. Similarly, experiments were performed using NucBlue™ staining (a Hoechst stain derivative and trademark from ThermoFisher). However, unlike DAPI and Hoechst 33258, NucBlue showed no difference in FLT across the length of chromosomes (Figure 3A, Supplementary table 1). NucBlue labels live cells DNA faster than Hoechst 33258 and DAPI, and have an excellent cell permeability. The use of NucBlue was unable to provide much information on the chromosome preparation fidelity- reproducibility and repeatability since the lifetime values do not change unlike that of DAPI and Hoechst 33258. Whilst this comparison compares FLT changes in human T cell chromosomes and investigates specifically the lifetime difference between the centromere and the chromosomal arms, it also demonstrates the sensitivity of different stains for FLIM imaging of chromosomes. DAPI showed the largest difference in lifetime of the stains investigated here, suggesting that it might also be the most sensitive to other changes in the micro and nano-environment for future work involving chromosome imaging.

Effect of DAPI concentration on fluorescent lifetime of metaphase chromosomes

The concentration effect of DAPI applied to chromosomes was examined using FLIM. Human T cell chromosomes were prepared and mounted onto slides and were subjected to different DAPI concentrations ranging from 0.04 µM to 400 µM. Chromosomes stained with different DAPI concentrations were FLIM imaged and the FLTs were acquired from the arms and heteromorphic centromeric region of chromosome 1. Chromosome 1 was selected as it is the largest chromosome and easy to identify. The results of these are shown in Figure 4, where the graph shows little to no difference in the DAPI FLT between 0.04 µM and 4 µM. Between 40 µM and 400 µM DAPI, there is no significant difference in DAPI FLT between the arms and centromeric region of chromosome 1. A T-test used to determine a difference in the centromeric and arm DAPI FLT, only found significance for 0.04, 0.4 and 4 µM DAPI, with significance values of < 0.001 apiece. Meanwhile, 40 µM and 400 µM had significance values

of 0.54 and 0.086 respectively, suggesting there is not a statistically significant difference between the chromosomal subregions (Supplementary figure 1A). However, between 4 µM and 400 µM there is a significant step-wise decrease in DAPI FLT of both the centromere and the chromosomal arms of the chromosomes. With a mean centromeric DAPI FLT of 2.712 ± 0.058 ns between 0.04 - 4 µM, compared to 1.31 ± 0.35 ns for 40 µM DAPI and 0.41 ± 0.03 ns for 400 µM DAPI. A two-way ANOVA (Supplementary figure 1B) and Tukey HSD Post-Hoc testing (Supplementary figure 1C) were used to determine the significance of the difference in the DAPI FLT means of the different concentrations. This found no significant difference between 0.04 and 4 µM DAPI. However, there was a clearly significant difference for all concentrations between 4 and 400 µM, with a significance value of <0.001. This is less than the significance threshold of 0.05, allowing the null hypothesis stating there is no significant difference to be rejected. This indicates there is a concentration effect seen for DAPI concentrations 40 µM and greater.

Following this chromosomes from different human and non-human cell lines were stained using 4 µM DAPI. A two-sample T test was used to compare the FLT of the arms and heteromorphic region of chromosome. A significant decrease is seen in the FLT at the heteromorphic region of chromosome one in human cell lines (Supplementary figure 2, A-C and F), whereas no significant difference was seen in non-human cell lines D) chinese hamster ovary (CHO) cells and E) Gerbil Spleen cells (Supplementary figure 2, D, and F). It is interesting to see an heteromorphic to arm FLT difference only in human cells and not in CHO or gerbil chromosomes. This may be due to sequence differences reported in human cells compared to non-human cells. This could indicate that other DNA binding fluorescence stains may be useful to examine in the future for non-human species for identifying FLT on chromosomes.

Changes of fluorescence lifetime due to drying effects of DAPI on fixed chromosomes

In order to evaluate and improve the influence of possible interactions between the fixation solution MAA and DAPI, a comparison was made between DAPI FLT and the drying time for chromosome preparations following mounting on glass slides and prior to staining. Chromosome samples are commonly preserved using MAA (Tobias et al. 2011). T cell chromosomes were prepared and mounted as described in earlier. 5 minutes allowed slides to partially dry and whilst 10 minutes drying time was already beyond that is generally used.

FLIM imaging of chromosome slides partially dried (5 minutes) prior to DAPI staining showed an average FLT of 2.1 ns. Whereas, slides allowed to dry completely (10 minutes) prior to DAPI staining gave a FLT of 3 ns (Figure 5). This latter value is similar to the chromosome bound DAPI lifetime of 2.95 ns that was found in previous FLIM chromosome studies (Estandarte et al, 2016). These results can be explained by considering the chemical properties of DAPI, so that in a partially dried MAA fixation solution is able to react with DAPI. DAPI has two amidine functional groups, which react with both alcohol and acids (Barcellona and Gratton, 1989). Therefore, it is assumed that DAPI would react with the MAA fixation solution and as a result its fluorescent properties may change. Here, the reaction with MAA results in a quenching of DAPI's fluorescent properties, leading to a lower FLT than in the absence of any chemical reaction. Therefore, lifetime measurement can be a simple way to adjust the preparation of chromosome slides to ensure that slides are completely dried after mounting prior to staining, to ensure that any difference in FLT is reproducible and not influenced by large variation sample preparation.

Effect of hydration on measurements of chromosome FLT

As mentioned previously the acquisition of good FLIM images relies on the level of photon count during the imaging process. Low photon counts require long acquisition times which may lead to sample photo-bleaching. One source of low photon counts is due to dry chromosome samples on the glass slide. Therefore, an investigation was carried out to compare the image characteristics taken of dehydrated slides versus slides where water was added underneath the coverslip to rehydrate the slide. The coverslip can simply be hydrated by placing a drop of purified water against the edge of the coverslip and allowing it to spread underneath the coverslip until the entire surface area is covered. It was found that in images where the coverslip was not hydrated (Figure 6), there was a poorer photon count and FLIM resolution. The deterioration in image quality is not surprising since most high numerical aperture (>1) microscope objectives require an immersion media such as water, oil or glycerol. The sample therefore needs to match this media. In our experiments, we have used a 60x, water NA 1.2 microscope objective. The photon counts will also be reduced since the full NA (or angle of light collection from the sample) is reduced. Moreover, the lifetime was decreased from the literature DAPI FLT of 2.95 ns (Bhartiya et al, 2021) and from the wet chromosome FLT of an average of ~3 ns (Figure 6a) to an average FLT of ~2.85 ns when the sample was dry (after ~5

hours); (Figure 6b). This is also represented in the distribution graph (Figure 6C). It is worth noting that this reduction in lifetime is not a consequence of the microscope NA but rather a good indication of the chromosome preparation quality and structural characteristics that are missing from the dried chromosome. This suggests that dried chromosomal DNA is somewhat different to that of a fully hydrated one. This shows a significant decrease from the expected lifetime value and indicates that chromosome drying up has a noticeable effect on the chromosome structure and is reported by the fluorescent properties of DAPI. This effect is generally by rehydrating the sample. Hence this represents a need to continuously monitor the mounting slide throughout imaging, with coverslip hydration representing one of the first factors to check if unexpected lifetimes are being found. Again, the use of FLT is an excellent way to monitor the structural changes taking place during the imaging process. As this identifiable difference in FLT in response to this sample preparation step might accidentally be identified as a significant FLT difference if this is not considered. As often throughout extended periods of imaging, the slide can begin to dehydrate.

Ionising radiation causes noticeable changes in the heteromorphic regions of chromosomes

Once the physical parameter for the optimisation process was established, we proceeded to test the effects of DNA damaging agent and analysis using FLIM. Mammalian HeLa cells were irradiated with a range of x-ray does, 0, 0.1, 0.5 and 1 Gy. Chromosomes were prepared using the newly improved and optimised protocol. Since mammalian cell chromosome 1 is known to be the largest chromosome in the human genome, identification was easier than the rest. We found that the heteromorphic region of this DAPI labelled chromosome 1 reduced from 2.7 ns to 2.1 ns following live cells ionising radiation with 0.1 to 0.5 Gy, respectively (Figure 7). The reason for this change is novel and unknown. There is no statistical difference in the lifetime of cells irradiated with 0.1 Gy and 1 Gy (Supplementary Figure 3). However, both HeLa (Supplementary Figure 3) and human T cells (Supplementary Figure 4) show a significant difference in the lifetime between cells irradiated at 0.5 Gy and all other doses (0, 0.1 and 1 Gy).

Our improved chromosome preparation allowed these changes to be easily observed. Clear FTL differences between 0.1, 0.5 and 1 Gy can be seen in Supplementary figure 5A with improved sample preparation. whereas random sample preparation parameters showed a

variation in FLT with a larger standard deviation and reduction in FLT after irradiation (0.1, 0.5 and 1 Gy) as in Supplementary figure 5B. Random sample preparation gives a poor prognosis due to improper drying of MAA fixation, or inappropriate concentration of DAPI and chromosome dehydration. The reduction of FLT at 0.5 Gy can only be observed with the improved sample preparation conditions highlighting the need for careful preparations before any experiment.

Radiobiological studies have shown a surviving fraction of ~90 % for 1 Gy dose. However, a number of reports have reported hypersensitivity below 0.8 Gy with a surviving fraction of close to 80%. (Joiner et al, 2001). However, there is also a significant radiation dose effect around 0.2- 0.7 Gy). The reason for this increased sensitivity below 0.7 Gy for cell survival is unknown. It is interesting to note that a difference in the lifetime of the heteromorphic region at doses below 1 Gy. We there speculate that there may be a link between the hypersensitivity previously observed and what we observe in this study. Indeed radiotherapy irradiations with 0.5 Gy fractions has been suggested as a more effective way of providing radiotherapy utrafractionation' (Lambin et al, 1993).

As mentioned in the introduction, chromosomes also undergo instability and a range of other changes, known as aberrations. These include both structural changes and chromosome number (loss or gain). Structural changes generally manifest as translocations, deletions, inversions and exchanges between different chromosomes. These are normally identified following chromosome preparations and mFISH assays. Although we have not performed a mFISH assay here, we are able to identify chromosome 1 readily by size and the unique feature of reduced centromere lifetime against the rest of the chromosome arm and other chromosomes. It is thought that the cell centromere critically assembles the kinetochore and maintains sister chromatids co-localisation prior to chromosome separation. Defects in these functions may lead to lagging chromosomes, aneuploidy and micronuclei. Centromeres are difficult to study due to their repetitive base sequence. The change in lifetime observed using FLIM may be a valuable tool in investigating their function.

Decondensation of polyamine chromosomes represent lifetimes similar to fixed chromosomes

We measured DAPI lifetime of 'in-solution' polyamine chromosomes whose structures were not fixed with MAA. The change of DAPI lifetime of these chromosomes was monitored

upon the treatment with EDTA-HEPES that decondensed chromosomes. At the beginning where chromosomes were kept in PA buffer, the average lifetime of the whole chromosomes was 2.8 ± 0.1 ns (Figure 8 A)which was shorter than MAA chromosomes that had a lifetime of 3.1 ns (???) . We were able to detect different lifetime between heteromorphic (2.5 ns) and arm (2.7 ns) regions in PA chromosomes (Figure 8 C). Treatment with EDTA-HEPES, a cation chelator, induced chromosome decondensation, resulting in the increase of average lifetime to 3.1 ± 0.1 ns (Figure 8B) and 2.8 ns for heteromorphic region and 3.0 ns for arm region (Figure 8D). The lifetime of decondensed chromosomes was comparable to the MAA chromosomes. We speculate that the native chromosomes are the most compact state therefore the lifetime was the shortest. With MAA fixation, chromosomes were enlarged and flattened when contacting the slide surface during chromosome spread preparation. MAA prepared chromosomes are decondensed as part of the histones are removed (Sumner et al, 1973; Sone et al, 2002). In comparison, human polyamine chromosomes retain both their proteins and nucleic acid after preparation (Lewis & Laemmli, 1982) making them shorter and highly condensed. As MAA fixed chromosomes partially reduce the degree of compaction, we observed longer lifetime in the MAA chromosome, similar to the 'in-solution' decondensed chromosomes.

A summary of FLT for all different chromosome preparation conditions is in Supplementary figure 6.

Conclusions

The importance of sample preparation in chromosome research is vital for cell health and medical research. Here we aimed to critically investigate and highlight experimental factors that influence the current chromosome preparation and imaging protocol. We identified a number of optimised procedures and applied them to human cell lines, focusing primarily on the following steps; fixation process, chromosome mounting on slides, staining with DNA localisation probes and imaging conditions. Although this study specifically focuses on the optimisation of chromosome sample preparation for the use in FLIM, this in turn, informed on the quality of the chromosomes prepared. Using the FLIM technique together with the optimised process, we show that imaging of prepared chromosome slides should be imaged ideally after staining, whilst the coverslips should be hydrated throughout the duration of

imaging. Moreover, DAPI was found to be a more sensitive probe for FLIM than Hoechst and its derivatives. No cell line difference was found, indicating that the new improvements are applicable to most human cell lines. While this study focused on the impact of these optimisations of FLIM, many of the optimisation explored have potential for other microscopy techniques such as epifluorescence, confocal and super resolution. The latter, with a resolution of 10-100 nm, demands careful and excellent chromosome preparation techniques to determine the true structure. The technique improvements identified allowed determination of changes in the chromosome heteromorphic region following ionising radiation thus opening a new research direction for chromosome compaction and structure which are difficult to study.

Acknowledgements

This work is supported by UKRI- STFC, funding access to the Central Laser Facility (SWB IM research, We are grateful for Drs Sylwia Kabacik who performed the x-ray irradiations. Work performed at UCL was supported by a BBSRC Professorial Fellowship. For the purpose of open access, the authors have applied a Creative Commons Attribution (CC BY) licence to any Author Accepted Manuscript version arising.

References

Ahmed, A., Schoberer, J., Cooke, E., & Botchway, S. W. (2021). *Multicolor FRET-FLIM Microscopy to Analyze Multiprotein Interactions in Live Cells*. 287–301. https://doi.org/10.1007/978-1-0716-1126-5_16

Barcellona, M. L., & Gratton, E. (1989). Fluorescence lifetime distributions of DNA-4′,6-diamidino-2-phenylindole complex. *Biochimica et Biophysica Acta (BBA) - General Subjects*, *993*(2–3), 174–178. https://doi.org/10.1016/0304-4165(89)90160-8

Bhartiya, A., Batey, D., Cipiccia, S., Shi, X., Rau, C., Botchway, S., Yusuf, M., & Robinson, I. K. (2021). X-ray Ptychography Imaging of Human Chromosomes After Low-dose Irradiation. *Chromosome Research*, *29*(1), 107–126. https://doi.org/10.1007/s10577-021-09660-7

Binz, R. L., Burns, K., & Pathak, R. (2024). Protocol for preparation and staining of chromosomes isolated from mouse and human tissues for conventional and molecular cytogenetic analysis. *STAR Protocols*, *5*(1), 102897. https://doi.org/10.1016/j.xpro.2024.102897

Botchway, S. W., Farooq, S., Sajid, A., Robinson, I. K., & Yusuf, M. (2021). Contribution of advanced fluorescence nano microscopy towards revealing mitotic chromosome structure. *Chromosome Research*. https://doi.org/10.1007/s10577-021-09654-5

Botchway, S. W., Parker, A. W., Bisby, R. H., & Crisostomo, A. G. (2008). Real-time cellular uptake of serotonin using fluorescence lifetime imaging with two-photon excitation. *Microscopy Research and Technique*, *71*(4), 267–273. https://doi.org/10.1002/jemt.20548

Botchway, S. W., Scherer, K. M., Hook, S., Stubbs, C. D., Weston, E., Bisby, R. H., & Parker, A. W. (2015). A series of flexible design adaptations to the Nikon E-C1 and E-C2 confocal microscope systems for UV, multiphoton and FLIM imaging. *Journal of Microscopy*, *258*(1), 68–78. https://doi.org/10.1111/jmi.12218

Breusegem, S. Y., Clegg, R. M., & Loontiens, F. G. (2002). Base-sequence specificity of Hoechst 33258 and DAPI binding to five (A/T)4 DNA sites with kinetic evidence for more than one high-affinity Hoechst 33258-AATT complex. *Journal of Molecular Biology*, *315*(5), 1049–1061. https://doi.org/10.1006/jmbi.2001.5301

Cavatorta, P., Masotti, L., & Szabo, A. G. (1985). A time-resolved fluorescence study of 4′,6′-diamidine-2-phenylindole dihydrochloride binding to polynucleotides. *Biophysical Chemistry*, *22*(1–2), 11–16. https://doi.org/10.1016/0301-4622(85)80021-1

Clancy, E., Ramadurai, S., Needham, S. R., Baker, K., Eastwood, T. A., Weinstein, J. A., Mulvihill, D. P., & Botchway, S. W. (2023). Fluorescence and phosphorescence lifetime imaging reveals a significant cell nuclear viscosity and refractive index changes upon DNA damage. *Scientific Reports*, *13*(1), 422. https://doi.org/10.1038/s41598-022-26880-x

Estandarte, A. K., Botchway, S., Lynch, C., Yusuf, M., & Robinson, I. (2016). The use of DAPI fluorescence lifetime imaging for investigating chromatin condensation in human chromosomes. *Scientific Reports*, *6*(31417), 1–12. https://doi.org/10.1038/srep31417

Haraguchi, T., Kaneda, T., & Hiraoka, Y. (1997). Dynamics of chromosomes and microtubules visualized by multiple-wavelength fluorescence imaging in living mammalian cells: effects of mitotic inhibitors on cell cycle progression. *Genes to Cells*, *2*(6), 369–380. https://doi.org/10.1046/j.1365-2443.1997.1280326.x

Hayashihara, K., Uchiyama, S., Kobayashi, S., Yanagisawa, M., Matsunaga, S., & Fukui, K. (2008). Isolation method for human metaphase chromosomes. *Protocol Exchange*. https://doi.org/10.1038/nprot.2008.166

HSU, T. C. (1952). MAMMALIAN CHROMOSOMES IN VITRO. *Journal of Heredity*, *43*(4), 167–172. https://doi.org/10.1093/oxfordjournals.jhered.a106296

Huang, R., & Zhou, P.-K. (2021). DNA damage repair: historical perspectives, mechanistic pathways and clinical translation for targeted cancer therapy. *Signal Transduction and Targeted Therapy*, *6*(1), 254. https://doi.org/10.1038/s41392-021-00648-7

Hughes, A. (1952). Some Effects of Abnormal Tonicity on Dividing Cells in Chick Tissue Cultures. *Journal of Cell Science*, *S3-93*(22), 207–219. https://doi.org/10.1242/jcs.s3-93.22.207

Hungerford, D. A. (1965). Leukocytes Cultured from Small Inocula of Whole Blood and the Preparation of Metaphase Chromosomes by Treatment with Hypotonic KCL. *Stain Technology*, *40*(6), 333–338. https://doi.org/10.3109/10520296509116440

Jana, A., Crowston, B. J., Shewring, J. R., McKenzie, L. K., Bryant, H. E., Botchway, S. W., Ward, A. D., Amoroso, A. J., Baggaley, E., & Ward, M. D. (2016). Heteronuclear Ir(III)–Ln(III) Luminescent Complexes: Small-Molecule Probes for Dual Modal Imaging and Oxygen Sensing. *Inorganic Chemistry*, *55*(11), 5623–5633. https://doi.org/10.1021/acs.inorgchem.6b00702

Joiner, M. C., Marples, B., Lambin, P., Short, S. C., & Turesson, I. (2001). Low-dose hypersensitivity: current status and possible mechanisms. *International Journal of Radiation Oncology*Biology*Physics*, *49*(2), 379–389. https://doi.org/10.1016/S0360-3016(00)01471-1

Lambin P., Malaise E.P., & Joiner M.C. (1993). Megafractionnement: Une methode pour agir sur les tumeurs intrinsequement radioresistantes? *Bulletin Du Cancer. Radiothérapie*, *80*(4), 417–423.

Lewis, C. D., & Laemmli, U. K. (1982). Higher order metaphase chromosome structure: Evidence for metalloprotein interactions. *Cell*, *29*(1), 171–181. https://doi.org/10.1016/0092-8674(82)90101-5

Llères, D., James, J., Swift, S., Norman, D. G., & Lamond, A. I. (2009). Quantitative analysis of chromatin compaction in living cells using FLIM–FRET. *The Journal of Cell Biology*, *187*(4), 481–496. https://doi.org/10.1083/jcb.200907029

Makino, S., & Nishimura, I. (1952). Water-Pretreatment Squash Technic: A New and Simple Practical Method for the Chromosome Study of Animals. *Stain Technology*, *27*(1), 1–7. https://doi.org/10.3109/10520295209105053

Moralli, D., Yusuf, M., Mandegar, M. A., Khoja, S., Monaco, Z. L., & Volpi, E. V. (2011). An Improved Technique for Chromosomal Analysis of Human ES and iPS Cells. *Stem Cell Reviews and Reports*, *7*(2), 471–477. https://doi.org/10.1007/s12015-010-9224-4

Phengchat, R., Takata, H., Morii, K., Inada, N., Murakoshi, H., Uchiyama, S., & Fukui, K. (2016). Calcium ions function as a booster of chromosome condensation. *Scientific Reports*, *6*(1), 38281. https://doi.org/10.1038/srep38281

Portugal, J., & Waring, M. J. (1988). Assignment of DNA binding sites for 4′,6-diamidine-2-phenylindole and bisbenzimide (Hoechst 33258). A comparative footprinting study. *Biochimica et Biophysica Acta (BBA) - Gene Structure and Expression*, *949*(2), 158–168. https://doi.org/10.1016/0167-4781(88)90079-6

Rønne, M. (1990). Chromosome preparation and high resolution banding (review). *In Vivo (Athens, Greece)*, *4*(6), 337–365.

Sumner, A. T. (1982). The nature and mechanisms of chromosome banding. *Cancer Genetics and Cytogenetics*, *6*(1), 59–87. https://doi.org/10.1016/0165-4608(82)90022-X

Sumner, A. T., Evans, H. J., & Buckland, R. A. (1973). Mechanisms involved in the banding of chromosomes with quinacrine and Giemsa. *Experimental Cell Research*, *81*(1), 214–222. https://doi.org/10.1016/0014-4827(73)90128-6

Takefumi SONE, Megumi IWANO, Shouhei KOBAYASHI, Takeshi ISHIHARA, Naoto HORI, Hideaki TAKATA, Tatsuo USHIKI, S. U. nad K. F. (2002). Changes in Chromosomal Surface Structure by Different Isolation Conditions. *Arch. Histol. Cytol*, *65 (5)*, 445–455. http://www2.kobe-u.ac.jp/~ohmido/Ohmido Lab/CL2003/pdf/03AHC_TS.pdf

Tanious, F. A., Veal, J. M., Buczak, H., Ratmeyer, L. S., & Wilson, W. D. (1992). DAPI (4',6-diamidino-2-phenylindole) binds differently to DNA and RNA: minor-groove binding at AT sites and intercalation at AU sites. *Biochemistry*, *31*(12), 3103–3112. https://doi.org/10.1021/bi00127a010

Therman, E. (1980). Structure of the Eukaryotic Chromosome and the Karyotype. In *Human Chromosomes* (pp. 11–23). Springer US. https://doi.org/10.1007/978-1-4684-0107-3_2

Tobias, E. S., Connor, M., & Ferguson-Smith, M. (2011). Essential Medical Genetics, Includes Desktop Edition. In *John Wiley & Sons*.

Visvanathan, A., Ahmed, K., Even-Faitelson, L., Lleres, D., Bazett-Jones, D. P., & Lamond, A. I. (2013). Modulation of Higher Order Chromatin Conformation in Mammalian Cell Nuclei Can Be Mediated by Polyamines and Divalent Cations. *PLoS ONE*, *8*(6), e67689. https://doi.org/10.1371/journal.pone.0067689

Yusuf, M., Leung, K., Morris, K. J., & Volpi, E. V. (2013). Comprehensive cytogenomic profile of the in vitro neuronal model SH-SY5Y. *Neurogenetics*, *14*(1), 63–70. https://doi.org/10.1007/s10048-012-0350-9

Yusuf, M., Parmar, N., Bhella, G. K., & Robinson, I. K. (2014). A simple filtration technique for obtaining purified human chromosomes in suspension. *BioTechniques*, *56*(5), 257–261. https://doi.org/10.2144/000114168

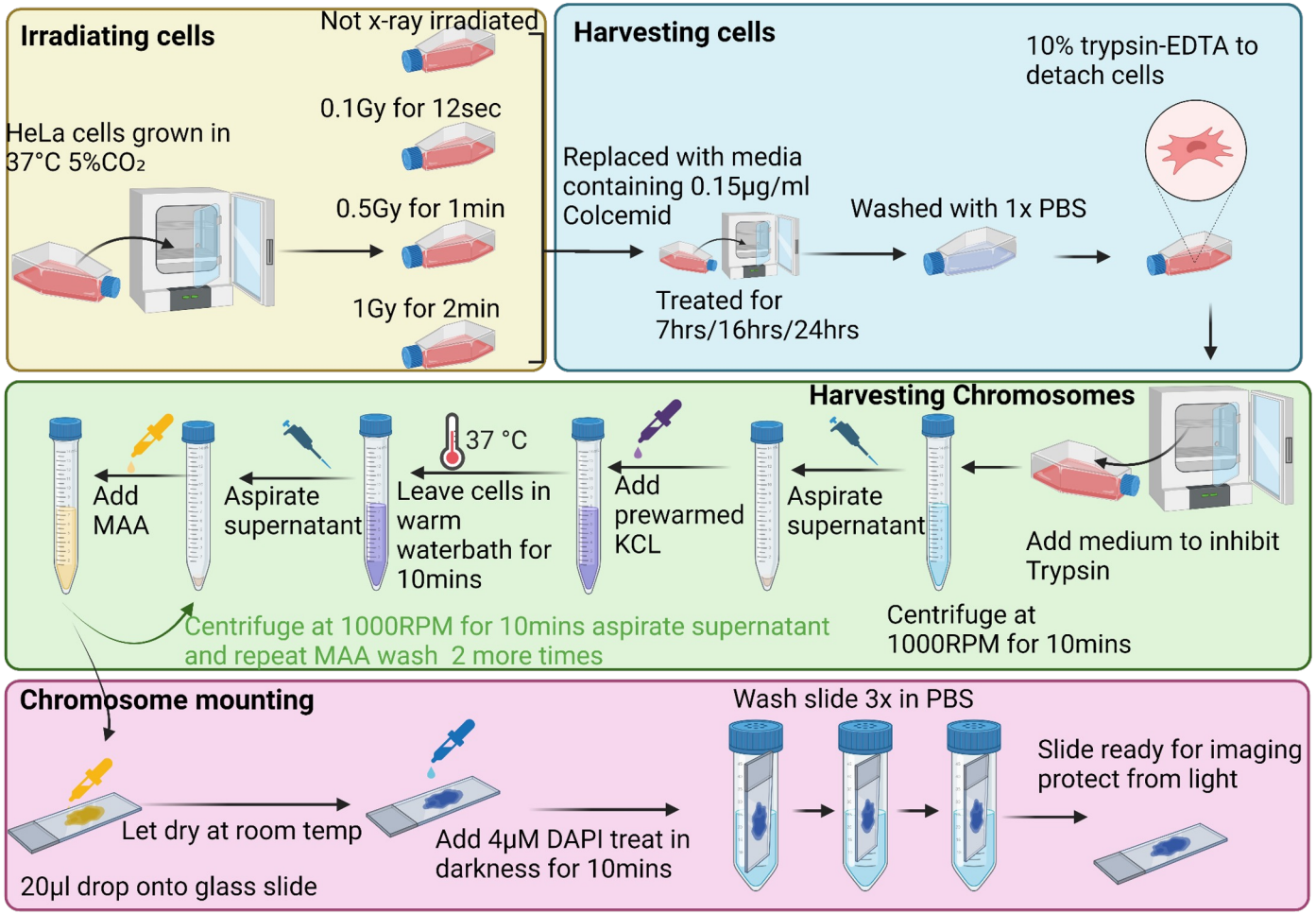

Figure 1. A. Flow diagram showing preparation of chromosomes including irradiation steps.

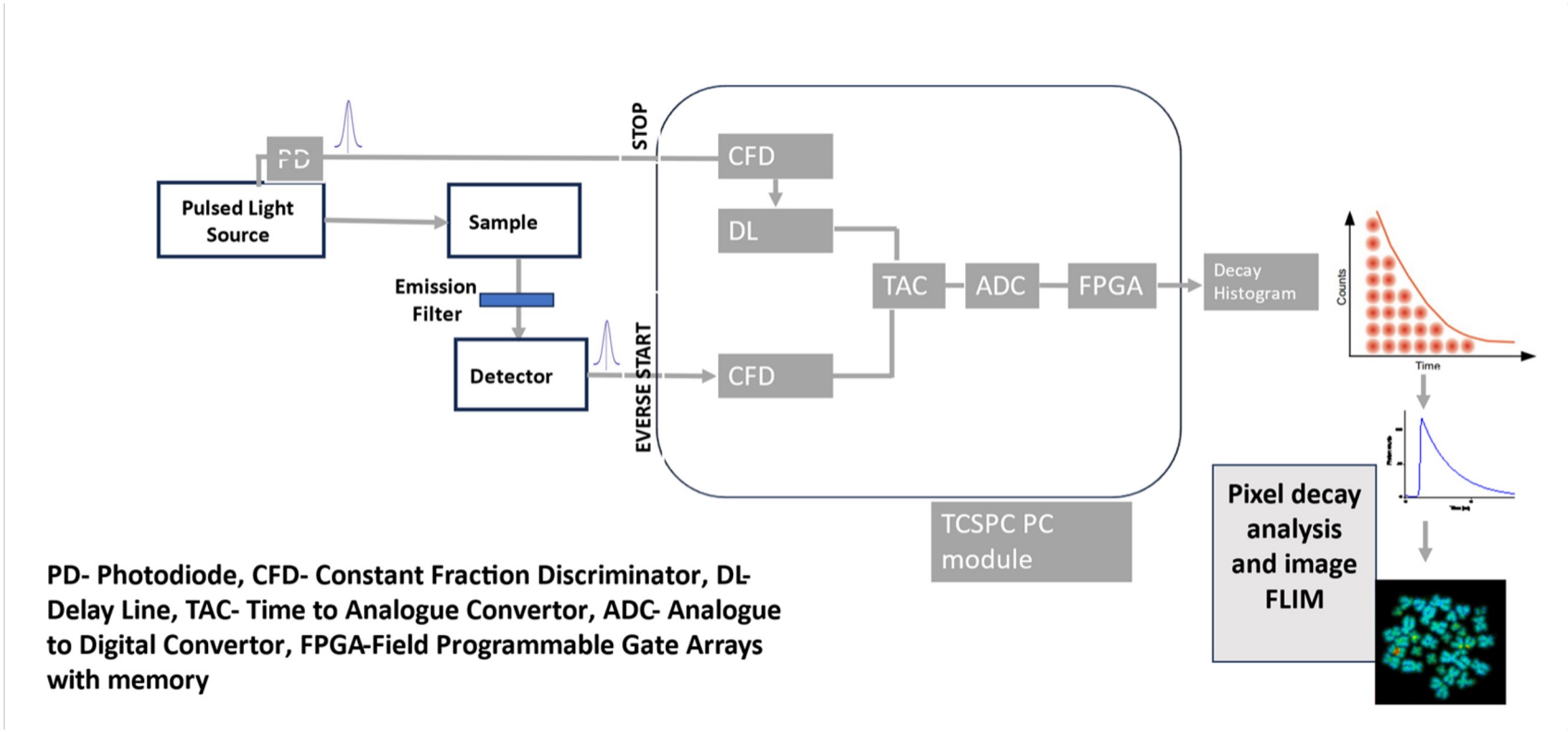

Figure 2. Schematic of multiphoton excitation FLIM with a confocal laser scanning microscopy setup. Sub-nanosecond excited state lifetime measurements using time-correlated single photon counting, TCSPC.

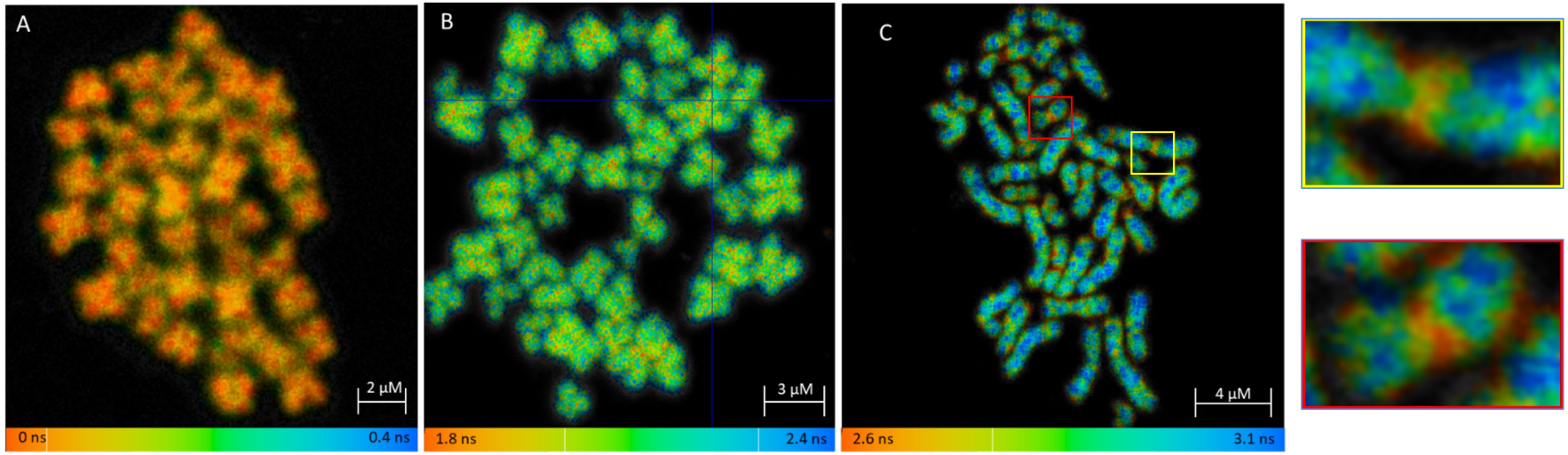

Figure 3. Comparison of different DNA fluorescence stains for fluorescence lifetime imaging microscopy of chromosomes. Comparison of FLIM T cell chromosome spreads stained with A) NucBlue B) Hoechst 33258 and C) DAPI and imaged using 405 nm FLIM excitation.
The fluorescent lifetime represented by the colour scales is displayed underneath each image A, B and C
A) NuncBlue resulted no arm/centromere lifetime difference
B) Hoechst resulted in a lifetime of 2.1 ns with no clear arm to centromere lifetime difference.
C) DAPI resulted in clear arm (3.1 ns) and centromere (2.6 ns) lifetime differences on individual chromosomes. 2 separate chromosomes are shown in the red and yellow box.

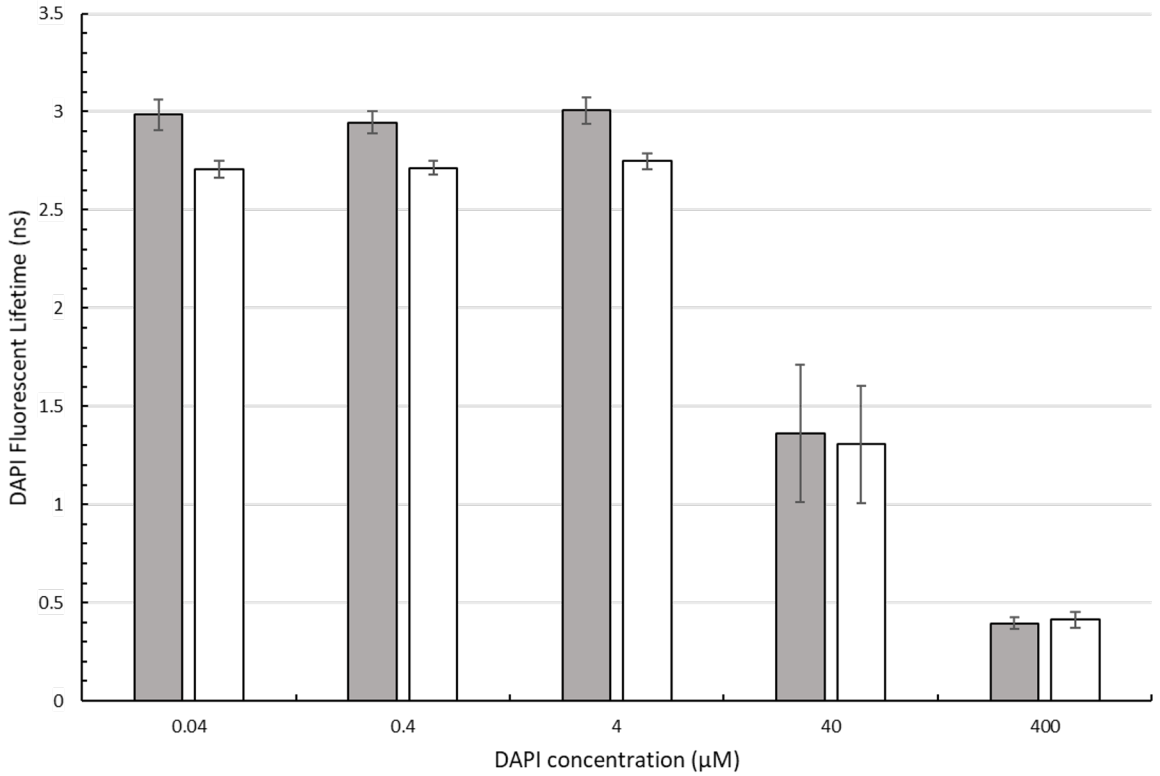

Figure 4: Clustered bar graph showing the effect of different DAPI concentrations on the DAPI fluorescence lifetime of human T cell chromosomes: Chromosomes were stained with different DAPI concentrations between 0.04 and 400 µM. With grey bars showing the fluorescent lifetime of the arms of chromosome 1 and white bars showing the fluorescent lifetime of the shorter heteromorphic region of chromosome 1. Error bars represent the standard deviation within each data set, with each bar calculated from 5 random pixels within each subregion, from 5 distinct chromosome spreads.

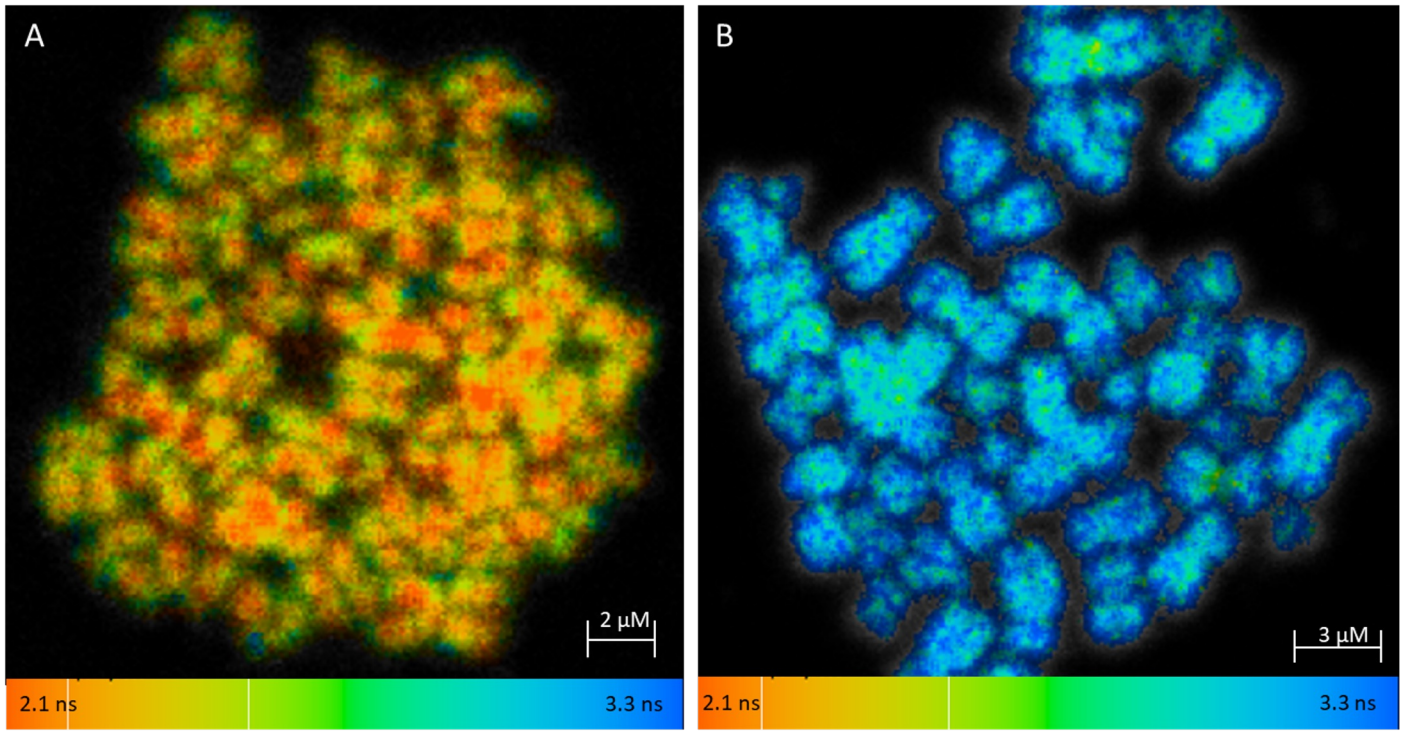

Figure 5. Methanol:acetic acid effect and interactions with chromosome labelled DAPI fluorescent lifetime. Chromosome preparation mounted onto slides, either partially (A) or fully (B) dried after MAA treatment and stained with 4 µM DAPI. Chromosome spreads were FLIM imaged using 405 nm excitation. The FLT is represented by the colour scales displayed underneath each image, with blue representing a longer fluorescent lifetime around 3 ns and orange representing a low fluorescent lifetime around 2.1 ns.

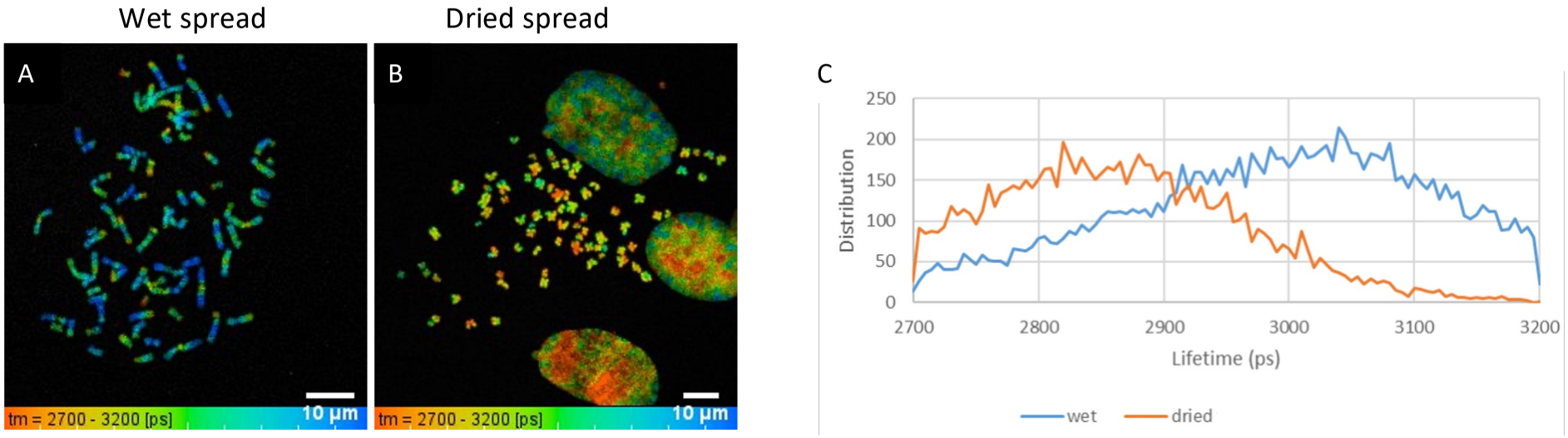

Figure 6. Importance of coverslip hydration and effect on chromosome FLT.
A) Wet HeLa chromosome spread has a FLT ~3 ns B) Dried HeLa chromosome spread has a FLT of ~2.85 ns. Dried images were acquired after ~5 hours of slide preparation. C) Distribution of FLT between wet and dried chromosome spreads.

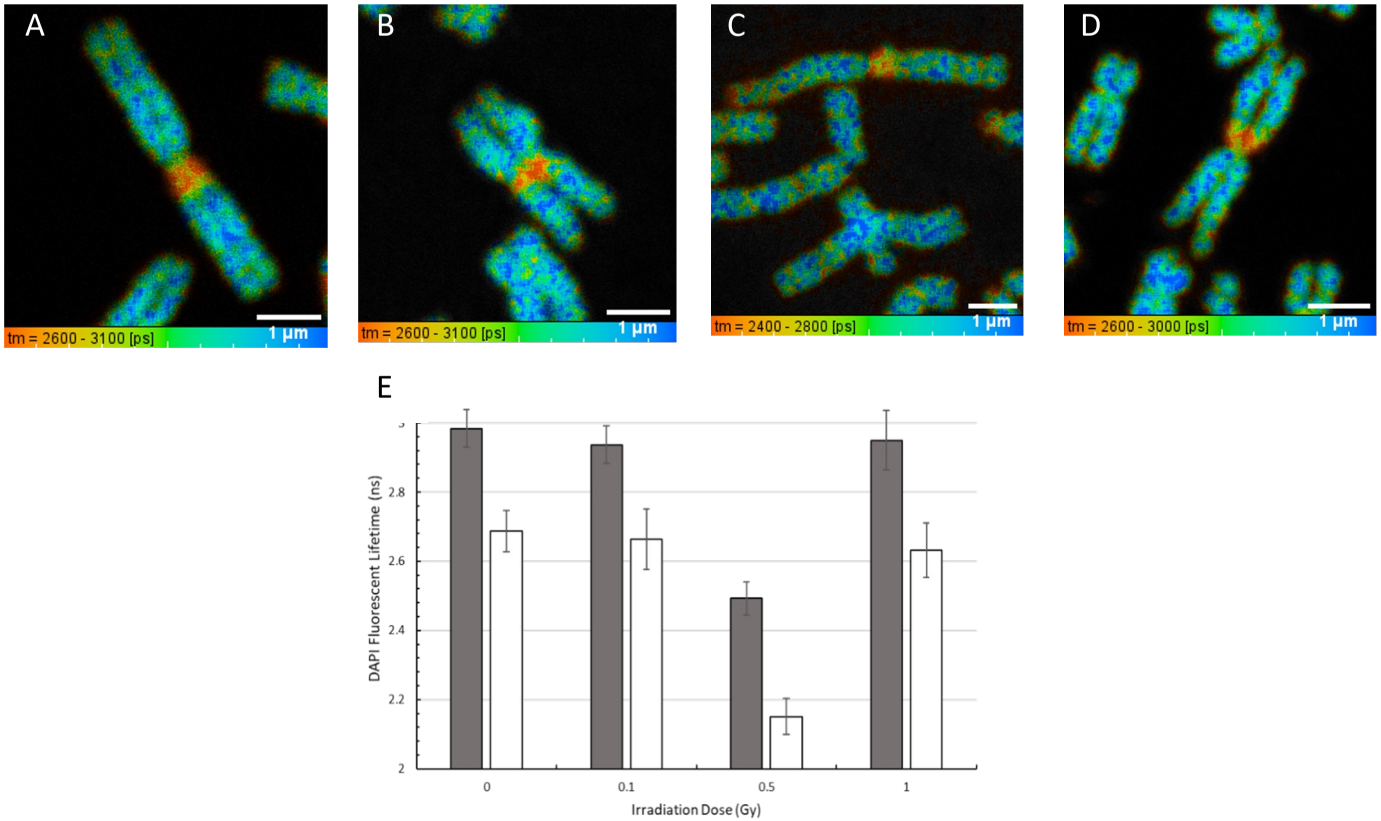

Figure 7. DAPI FLT of chromosomes after different x-ray irradiation doses. FLT images of HeLa human chromosome 1 after different irradiation doses A) 0, B) 0.1, C) 0.5 and D) 1 Gy irradiation. E) Clustered bar graph showing the DAPI fluorescence lifetime of irradiated HeLa metaphase chromosomes. Grey bars show the FLT of the chromosome 1 arms where as white bars show the FLT of the heteromorphic regions. 60x water objective was used to image 5 spreads. The chromosome one's show a reduction in FLT when exposed to ionising irradiation with the shortest lifetimes measured at 0.5Gy and a FLT recovery at 1Gy.

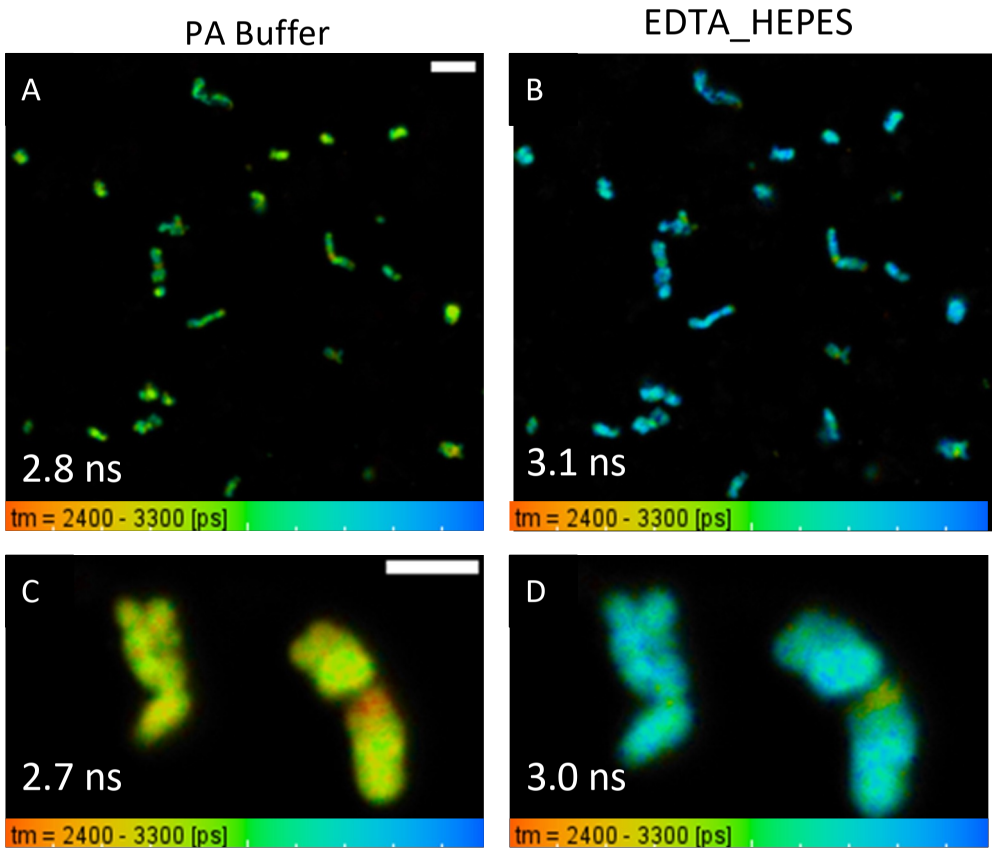

Figure 8. **Fluorescent Lifetime changes of 'in-solution' polyamine chromosomes.** Pseudocolor images of DAPI lifetime in chromosomes after chromosome decondensation. In lower panel, DAPI lifetime increased from 2.5 ns to 2.8 ns in heteromorphic regions, and 2.7 ns to 3.0 ns in arm regions. Scale bars = 5 μm (upper) and 2 μm (lower).

Supplementary Material

A) **2 Sample T-test of equal variance**

DAPI concentration	p Values
0.04 µM	4.11E-20
0.4 µM	4.26E-22
4 µM	1.8E-21
40 µM	0.540957
400 µM	0.085987

B) **Two-way ANOVA**

	Sum of Squares	df	Mean Square	F	Sig.
Between Groups	114.253	4	28.563	1476.381	0
Within Groups	2.322	120	0.019		
Total	116.574	124			

C **Tukey HSD post-Hoc testing**

(I) DAPI conc (uM)	(J) DAPI conc (uM)	Mean Difference (I-J)	Std. Error	Sig.	95% Confidence Interval	
					Lower Bound	Upper Bound
0.04 uM	0.4 uM	-0.004	0.03934	1	-0.113	0.105
	4 uM	-0.04	0.03934	0.847	-0.149	0.069
	40 uM	1.40320*	0.03934	0	1.2942	1.5122
	400 uM	2.29600*	0.03934	0	2.187	2.405
0.4 uM	0.04 uM	0.004	0.03934	1	-0.105	0.113
	4 uM	-0.036	0.03934	0.891	-0.145	0.073
	40 uM	1.40720*	0.03934	0	1.2982	1.5162
	400 uM	2.30000*	0.03934	0	2.191	2.409
4 uM	0.04 uM	0.04	0.03934	0.847	-0.069	0.149
	0.4 uM	0.036	0.03934	0.891	-0.073	0.145
	40 uM	1.44320*	0.03934	0	1.3342	1.5522
	400 uM	2.33600*	0.03934	0	2.227	2.445
40 uM	0.04 uM	-1.40320*	0.03934	0	-1.5122	-1.2942
	0.4 uM	-1.40720*	0.03934	0	-1.5162	-1.2982
	4 uM	-1.44320*	0.03934	0	-1.5522	-1.3342
	400 uM	.89280*	0.03934	0	0.7838	1.0018
400 uM	0.04 uM	-2.29600*	0.03934	0	-2.405	-2.187
	0.4 uM	-2.30000*	0.03934	0	-2.409	-2.191
	4 uM	-2.33600*	0.03934	0	-2.445	-2.227
	40 uM	-.89280*	0.03934	0	-1.0018	-0.7838

Supplementary figure 1: Statistical output for DAPI concentration fluorescence lifetime (FLT) comparison: Human T cells were prepared and mounted onto slides and were subjected to different DAPI concentrations ranging from 0.04 µM to 400 µM. FLT of the arms and hetromorphic regions of chromosome 1 was then determined using FLIM. In five different chromosome spreads, five random pixels within each region were selected and the mean FLT of each region calculated.

A) 2 Sample T-test of equal variance testing for differences in the FLT of the arms of centromeres of chromosome one, with a p-value of <0.05 suggesting a significant difference in FLT. **B)** Two-way ANOVA comparing the FLTs of the centromeric region at different DAPI concentrations (0.04 µM- 400 µM). Where a significance value of <0.05 suggests there is a difference between at least two of the DAPI concentrations. **C)** Tukeys HSD Post Hoc test to compare DAPI concentrations centromeric FLT against each other to test for significance between group comparisons. Where a significance value of <0.05 for a group comparison suggests there is a significance difference in the centromeric FLT at those DAPI concentrations.

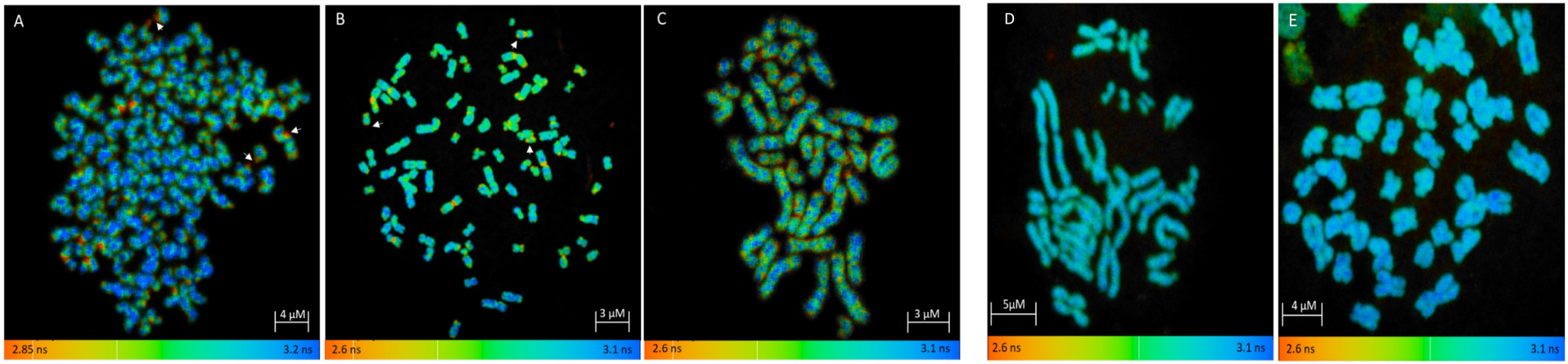

F)

Cell Line	p Value
HEK293T	6.78E-18
HeLa	7.46E-23
T cells	1.8E-21
CHO	0.43791
Gerbil Spleen	0.980812

Supplementary figure 2: FLIM images showing metaphase chromosome spreads from different human and non-human cell lines. Chromosomes were stained with 4 µM DAPI. With the cell lines used: **A)** HEK293T, **B)** HeLa, **C)** T cells, **D)** CHO cells and **E)** Gerbil Spleen cells. FLT is displayed using a false-colour scale bar. White arrows show examples of chromosomal aberrations. **F)** 2-sample T test showing differences in the FLT between the arms and heteromorphic regions of different human and non-human cell lines. Where a significance of <0.05 suggests there is a significant difference in the FLT of the arms and heteromorphic region. All human cell lines (**A-C**) show a decrease in FLT at the heteromorphic region of specific chromosomes within spreads, while no difference is seen in non-human cell lines (**D-E**).

A) **2 Sample T-test of equal variance**

Irradiation dose	p Values
control	7.46289E-23
0.1 Gy	9.94009E-18
0.5 Gy	1.60048E-28
1 Gy	4.61642E-18

B) **Two-way ANOVA**

	Sum of Squares	df	Mean Square	F	Sig.
Between Groups	4.918	3	1.639	327.67	0
Within Groups	0.48	96	0.005		
Total	5.398	99			

C **Tukey HSD post-Hoc testing**

(I) HeLa Condition (Gy)	(J) HeLa Condition (Gy)	Mean Difference (I-J)	Std. Error	Sig.	95% Confidence Interval	
					Lower Bound	Upper Bound
Control	0.1 Gy	0.0236	0.02001	0.641	-0.0287	0.0759
	0.5 Gy	.53640*	0.02001	0	0.4841	0.5887
	1 Gy	.05520*	0.02001	0.034	0.0029	0.1075
0.1 Gy	Control	-0.0236	0.02001	0.641	-0.0759	0.0287
	0.5 Gy	.51280*	0.02001	0	0.4605	0.5651
	1 Gy	0.0316	0.02001	0.395	-0.0207	0.0839
0.5 Gy	Control	-.53640*	0.02001	0	-0.5887	-0.4841
	0.1 Gy	-.51280*	0.02001	0	-0.5651	-0.4605
	1 Gy	-.48120*	0.02001	0	-0.5335	-0.4289
1 Gy	Control	-.05520*	0.02001	0.034	-0.1075	-0.0029
	0.1 Gy	-0.0316	0.02001	0.395	-0.0839	0.0207
	0.5 Gy	.48120*	0.02001	0	0.4289	0.5335

Supplementary Figure 3: Statistical output for different ionising radiation doses on the fluorescent lifetime of HeLa: HeLa cells were irradiated at different doses of ionising radiation ranging from 0 Gy to 1 Gy. From these irradiated cells, chromosomes were prepared and mounted onto slides and stained with 4 µM of DAPI. Fluorescent lifetime (FLT) of the arms and centromere of metaphase chromosome one was then determined using FLIM. In five different chromosome spreads, five random pixels within each region were selected and the mean FLT of each region calculated. **A)** 2 Sample T-test of equal variance testing for differences in the FLT of the arms of centromeres of chromosome one, with a p-value of <0.05 suggesting a significant difference in FLT. **B)** Two-way ANOVA comparing the FLTs of the centromeric region at different irradiation doses (0 Gy - 1 Gy). Where a significance value of <0.05 suggests there is a difference between at least two of the irradiation doses. **C)** Tukeys HSD Post Hoc test to compare irradiation doses centromeric FLT against each other to test for significance between group comparisons. Where a significance value of <0.05 for a group comparison suggests there is a significance difference in the centromeric FLT at those irradiation doses.

A) **2 Sample T-test of equal variance**

Irradiation dose	p Values
Control	1.801E-21
0.1 Gy	4.4902E-22
0.5 Gy	3.2318E-18
1 Gy	1.8137E-17

B) **Two-way ANOVA**

	Sum of Squares	df	Mean Square	F	Sig.
Between Groups	1.501	3	0.5	201.837	0
Within Groups	0.238	96	0.002		
Total	1.739	99			

C **Tukey HSD post-Hoc testing**

	(I) T cell Irradiation Dose (Gy)	(J) T cell Irradiation Dose (Gy)	Mean Difference (I-J)	Std. Error	Sig.	95% Confidence Interval	
						Lower Bound	Upper Bound
Tukey HSD	Control	0.1 Gy	.048000*	0.014081	0.005	0.01118	0.08482
		0.5 Gy	.312400*	0.014081	0	0.27558	0.34922
		1 Gy	.052520*	0.014081	0.002	0.0157	0.08934
	0.1 Gy	Control	-.048000*	0.014081	0.005	-0.08482	-0.01118
		0.5 Gy	.264400*	0.014081	0	0.22758	0.30122
		1 Gy	0.00452	0.014081	0.988	-0.0323	0.04134
	0.5 Gy	Control	-.312400*	0.014081	0	-0.34922	-0.27558
		0.1 Gy	-.264400*	0.014081	0	-0.30122	-0.22758
		1 Gy	-.259880*	0.014081	0	-0.2967	-0.22306
	1 Gy	Control	-.052520*	0.014081	0.002	-0.08934	-0.0157
		0.1 Gy	-0.00452	0.014081	0.988	-0.04134	0.0323
		0.5 Gy	.259880*	0.014081	0	0.22306	0.2967

Supplementary Figure 4: Statistical output for different ionising radiation doses on the FLT of T cells: Human T cells were irradiated at different doses of ionising radiation ranging from 0 Gy to 1 Gy. From these irradiated cells, chromosomes were prepared and mounted onto slides and stained with 4 µM of DAPI. FLT of the arms and heteromorphic region of chromosome one was then determined using FLIM. In five different chromosome spreads, five random pixels within each region were selected and the mean FLT of each region calculated. **A)** 2 Sample T-test of equal variance testing for differences in the FLT of the arms of centromeres of chromosome one, with a p-value of <0.05 suggesting a significant difference in FLT. **B)** Two-way ANOVA comparing the FLTs of the centromeric region at different irradiation doses (0 Gy - 1 Gy). Where a significance value of <0.05 suggests there is a difference between at least two of the

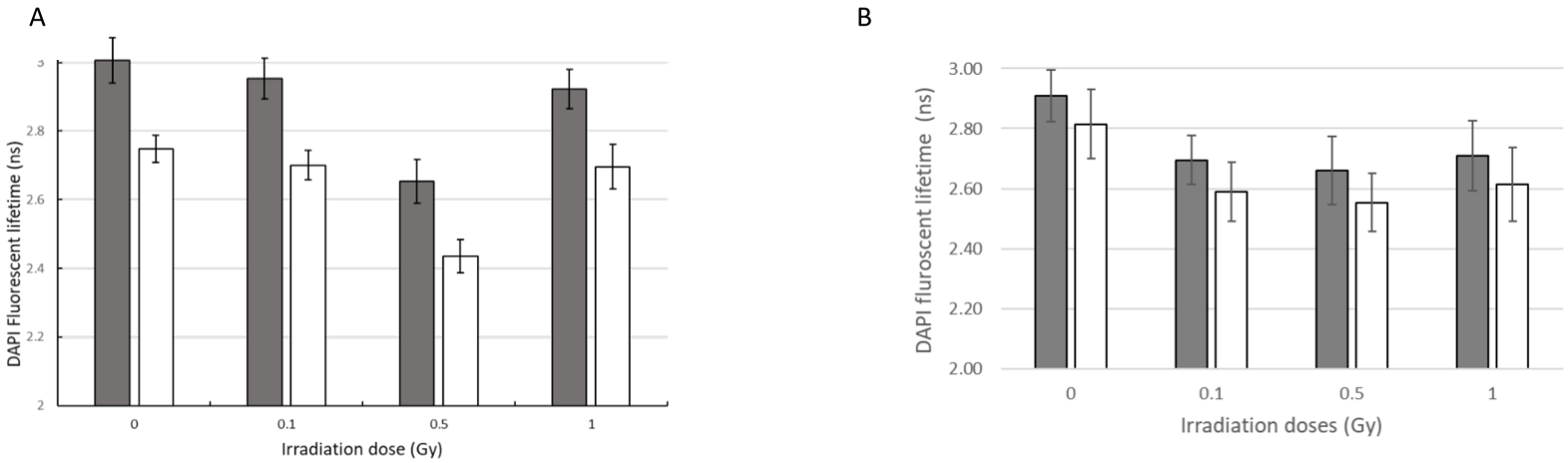

Supplementary figure 5. Represent DAPI FLT change of T cell chromosome 1's after different x-ray irradiation doses. A) Improved sample preparation (chromosome spreads n=5) and B) random sample preparation (chromosome spreads n = 9). 60x water objective was used for A and B.. Grey bars show the FLT of the chromosome 1 arms where as white bars show the FLT of the shorter heteromorphic regions of chromosome. Error bar represent standard deviation.

		Fluorescence Lifetime (ns)		
Condition	Cell type	Chromosome Arm	Heteromorphic region	Figures
NucBlue	HeLa	0-0.1	none	Figure 3A
Hoechst 33258	HeLa	2.1	none	Figure 3B
0.04-4 µM DAPI	Human T cells	3.1 - 3.2	2.6 - 2.7	Figure 3C and Figure 4
40 µM DAPI	Human T cells	1- 1.5	1- 1.4	Figure 4
400 µM DAPI	Human T cells	0.4	0.4	Figure 4
Wet Methanol Acetic Acid	Human T cells	2.1	none	Figure 5A
Dried Methanol Acetic Acid	Human T cells	3	2.7	Figure 5B
Wet Coverslip	HeLa	3.1-3.3	2.8-2.9	Figure 6A
Dried Coverslip	HeLa	2.9-3.0	2.7	Figure 6B
0 Gy ionising radiation	HeLa	3.0 - 3.1	2.6 - 2.7	Figure 7A and E
0.1 Gy ionising radiation	HeLa	2.9 - 3.0	2.6 - 2.7	Figure 7B and E
0.5 Gy ionising radiation	HeLa	2.4 - 2.5	2.1 - 2.2	Figure 7C and E
1 Gy ionising radiation	HeLa	2.8 - 3.0	2.6 - 2.7	Figure 7D and E
0 Gy ionising radiation	Human T cells	3.0 - 3.1	2.7 - 2.8	Supplementary Figure 5A
0.1 Gy ionising radiation	Human T cells	2.9 - 3	2.7	Supplementary Figure 5A
0.5 Gy ionising radiation	Human T cells	2.6 - 2.7	2.4 - 2.5	Supplementary Figure 5A
1 Gy ionising radiation	Human T cells	2.9 - 3.0	2.6 - 2.7	Supplementary Figure 5A
PA chromosome condensed	HeLA	2.7	2.5	Figure 8C
PA chromosome decondensed	HeLA	3.1	2.8	Figure 8D

Supplementary figure 6. Summary of FLT for different chromosome preparation conditions.